Journal of Sound and Vibration (1998) **214**(1), 57–66

OPTIMAL DESIGN TO REDUCE DYNAMIC INSTABILITY OF A TURBINE GENERATOR DUE TO MICROSLIP

H. L. WETTERGREN

Department of Mechanical Engineering, Linköping University, 58183 Linköping, Sweden

(*Received* 15 *May* 1996, *and in final form* 26 *January* 1998)

This paper is concerned with dynamic instability of a turbine generator due to friction between rotor slot wedges and the rotor. The energy transferred due to friction can be reduced by increasing wedge length, coefficient of friction or normal force or by reducing the cross-section area of the wedge. The bearing damping is normally sufficient to master the energy input from the wedges. This bearing damping becomes more powerful the weaker the bearings are. The size of the rotor cross-section area affected by the wedge is difficult to estimate but it is shown to be of minor importance for the results, provided it is larger than the wedge-cross-section area.

1. INTRODUCTION

For simple rotor systems there are some well-known basic reasons for instability, for instance non-conservative bearing stiffness forces, asymmetric shaft stiffness and internal damping. It is a well-known fact that when there is viscous damping in a rotating symmetrical shaft supported in symmetrical bearings, motion may be unstable above a certain speed, always above the lowest critical speed. The internal damping is however seldom viscous. A more common mechanism is the so-called microslip. The microslip phenomenon in rotordynamics was for the first time experimentally confirmed by Kimball [1] in a special test rotor with rings on hubs and shrunk on the shaft. Other papers in that subject are, for instance, those of Gunter [2] and Bently [3].

In this paper instability of a turbine generator due to this microslip will be studied; see Figure 1. The windings of turbine generators are built up in a number of axial slots milled in the rotor. The slots are rectangular and mostly in the radial direction to the rotor center. To hold the wound copper and the cooling pipes, rotor slot wedges are pressed into the slot.

When the generator is running microslip takes place between the wedges and the rotor. It is a well-known fact that when there is viscous or hysteretic damping in a rotating system instability may occur: see, for instance, references [4] and [5]. Friction models that include microslip have been derived since the 1950s [6]. Measuring microslip, however, is difficult because it is difficult to distinguish the elastic deformation of the contact from sliding in the contact. A good apparatus for measuring microslip has been developed by Hagman and Björklund [7].

In a previous paper Wettergren and Csaba [8] developed a method for tackling the microslip problem due to friction between the wedge and shaft in a turbine generator. They found that when the normal force on the wedge is constant the dissipated energy is of the same type as hysteretic material damping in the sense that for a circular motion excluding

0022–460X/98/260057 + 10 $25.00/0/sv981535

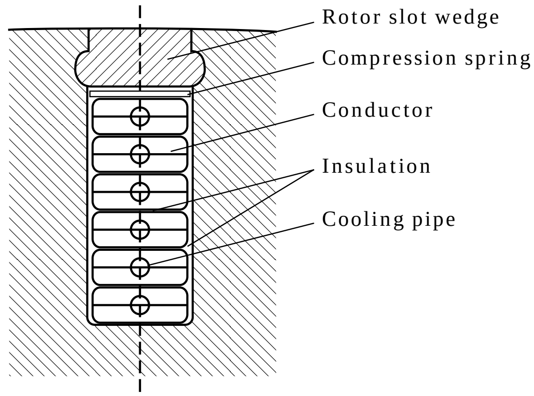

Figure 1. The winding of turbine generators.

gravity it is independent of the rotational frequency, but changes sign when the rotational frequency exceeds the vibrational frequency. The magnitude of the dissipated energy will however depend on the rotational frequency as the normal force does. The transferred energy due to friction is a non-linear phenomenon and approximately proportional to the amplitude cubed, and may be much larger than material damping. It was also shown that when gravity is included or the motion is elliptical the energy transferred is larger than for a simple circular motion.

The damping energy in the bearings is normally sufficient to master the energy transferred to the rotor from the wedge friction. This ratio is, however, affected by many design parameters, and cases may exist where the wedge friction is of decisive importance. Some of these design parameters will be investigated in this paper.

2. THE MODEL

A complete dynamic analysis of a turbine generator is complicated. The effects due to microslip can be isolated by drawing benefit from the knowledge that if the rotor becomes unstable it will start to vibrate with a frequency close to the first eigenfrequency. The vibration shape will be close to the first mode shape. Therefore the turbine generator can be reduced to a basic disc-shaft-bearing system; see Figure 2. The rotor system consists of a generalized mass, m, symmetrically mounted on a flexible shaft with the equivalent stiffness k_i obtained from the bending stiffnesses EI_1 and EI_2. The shaft is supported in two bearings with stiffness k_{ex} and k_{ey} and damping c_{ex} and c_{ey}. There are $n_{axial} \times n_{circ}$ wedges, where n_{axial} is the number of sets in the axial direction with n_{circ} wedges in the circumferential direction (a list of nomenclature is given in the Appendix).

In the microslip model one assumes that there is a part of the friction interface that slips, and another part that is stuck. The wedge and the rotor are shown in Figure 3. The wedge has modulus of elasticity E_w and cross-section area A_w. It is assumed to affect a part of the rotor having area A_r and modulus E_r.

The compression spring (see Figure 1) and the centrifugal acceleration exert a pressure on the wedge. The normal component of this pressure is assumed to give a constant distributed force q on the wedge. The friction force per unit length due to this normal force is defined upon using Coulomb friction as

$$F_f = \mu q. \tag{1}$$

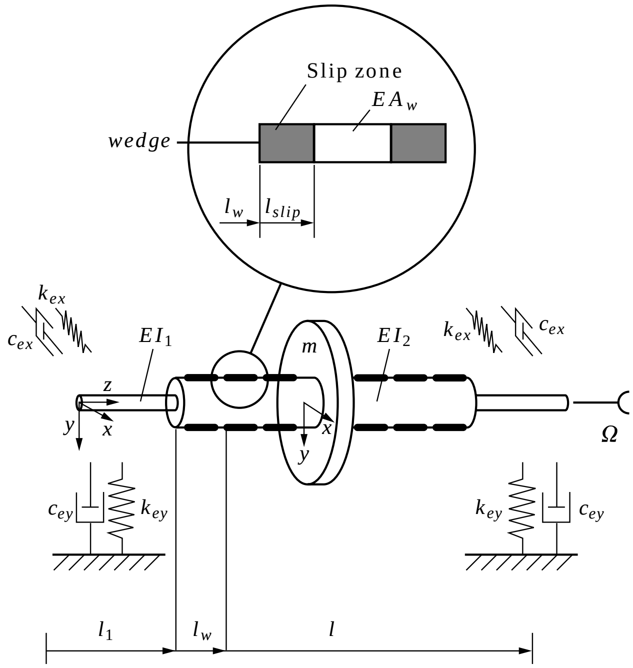

Figure 2. Simple rotor wedges.

Finally, the slip length δ_a is defined so that the strain in the wedge and the strain in the rotor are the same where the slip region ends.

The left part of one rotor wedge is shown in Figure 3.

Assume that just a part of the rotor is affected by the wedge. The additional bending moment on the rotor due to the wedge is the difference between the bending moment due to the force F and the corresponding bending moment if the wedge were not present. The forces required to force the rotor to perform circular motion can now be determined. This force due to the motion is illustrated in Figure 4.

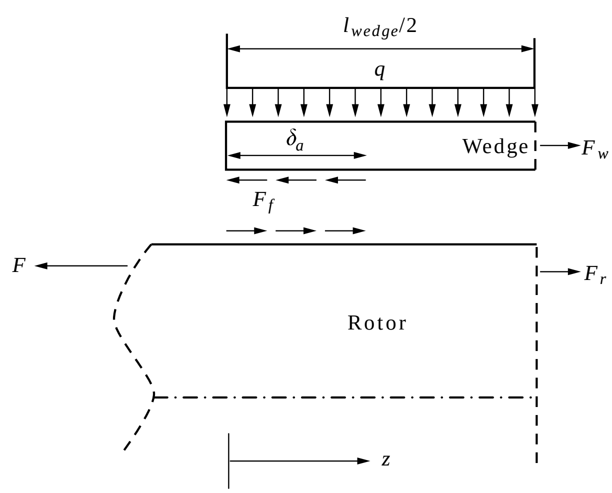

Figure 3. Forces acting on the left part of the wedge and the rotor.

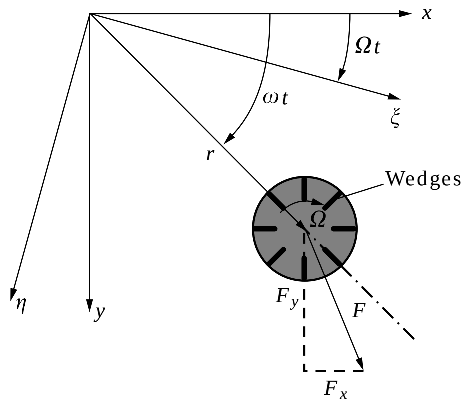

Figure 4. Deflection of the rotor.

If the forces on the rotor were purely elastic, they would be collinear with the deflection. The non-conservative nature of the microslip forces makes them have another direction: i.e., they add energy to the rotor or subtract energy from it. If energy is transmitted to the rotor instability may result.

The energy transferred to the rotor is

$$\Delta E = \int_{0 < \omega t \leqslant 2\pi} (F_x \, \mathrm{d}x + F_y \, \mathrm{d}y). \tag{2}$$

The energy transferred is compared with the total potential energy stored in the shaft. As the motion is circular and it fluctuates between a negative and a positive value the total potential energy becomes

$$E \approx 2k_i \, r_{max}^2, \tag{3}$$

where r_{max} is the maximal deflection of the shaft. The ratio between the energy dissipated and the elastic energy is in some sense a value of the damping in the shaft. The values for rotor materials, which can be used as a reference, are in the region of 0·01–0·1%.

3. RESULTS

Several simulations have been done using data from a real turbine generator. Details of the method used have been given by Wettergren and Csaba [8]. Without any ambition to describe quantitatively with a high degree of accuracy the behavior of a real turbine generator in this paper, which is mainly concerned with investigating the phenomenon in question, the following data are used as reference data from which the values may vary: the distance between the bearings, $l = 9{\cdot}2$ m; the generalized mass for the first eigenmode, $m = 37{,}363$ kg; the diameters of the shafts, $d_1 = 0{\cdot}7$ m, $d_2 = 1{\cdot}15$ m; the distance, $l_1 = 2{\cdot}25$ m. Except for the last calculation, the shaft is simply supported: i.e. $k_{ex} = k_{ey} = \infty$, $c_{ex} = c_{ey} = 0$. The number of wedges is chosen to be 36, i.e. $n_{circ} = 36$, and as before n_{axial} is equal to one. The length of the wedge is $l_{wedge} = 0{\cdot}6$ m. The friction coefficient is $\mu = 0{\cdot}1$ and the stiffness ratio is $\beta = (E_r A_r)/(E_w A_w) = 10$, where $E_w = 2{\cdot}06$ GPa and $A_w = 0{\cdot}0014$ m^2. The size of A_r is difficult to estimate, but it can be shown that it is of minor importance for the results, provided it is larger than A_w.

The normal force on the wedge depends on the prestressed spring between the wedge and the conductors and the centrifugal acceleration. When the rotational frequency exceeds a certain value the contact force between the conductors and the rotor vanishes and the normal force on the wedge becomes the sum of the centrifugal forces from the wedge and the conductors (see Figure 1). In these calculations the following contact forces are used:

$$N = F_{prestressed} + \frac{\rho_{wedge}\, l_{wedge}\, A_w\, d\Omega^2}{2 \sin \alpha_{wedge}}, \qquad \Omega \leqslant \omega_0^*,$$

$$N = \frac{m_{cond}\, r_{cond}\, \Omega^2}{\sin \alpha_{wedge}} + \frac{\rho_{wedge}\, l_{wedge}\, A_w\, d\Omega^2}{2 \sin \alpha_{wedge}}, \qquad \Omega > \omega_0^*, \tag{4}$$

where $F_{prestressed}$ is the force in the prestressed spring, α_{wedge} is the slope of the wedge contact area increasing when the wedge becomes less pointed, m_{cond} is the effective mass of the conductors, r_{cond} is the average radius where m_{cond} is applied and ω_0^* is the alteration frequency when the conductors lose the contact force from the rotor. In this paper the force in prestressed spring is equal to the centrifugal force for the conductors when $\Omega = \omega_e$: i.e. $\omega_0^* = \omega_e$ in this special case.

Let the mass perform a circular motion around the origin. To bring out the effects of the wedges the bearings are assumed to be rigid and the gravity force is ignored. Figure 5 shows how much energy per cylce is transferred to the system when the shaft is forced to make a revolution with the radius 0·001 m. Negative energy means that enery is added to the system and instability occurs. The average of 20 revolutions has been plotted.

From Figure 5 it is noted that instability may only occur when $\Omega > \omega_0$. A detailed discussion of how internal damping, such as friction, may cause instability can be found in Wettergren [9]. The energy transferred depends on Ω/ω_0 and it changes sign when Ω passes through ω_0. When the normal force is constant, however, the energy transferred is constant except that it changes sign when Ω passes through ω_0, analogously with material damping.

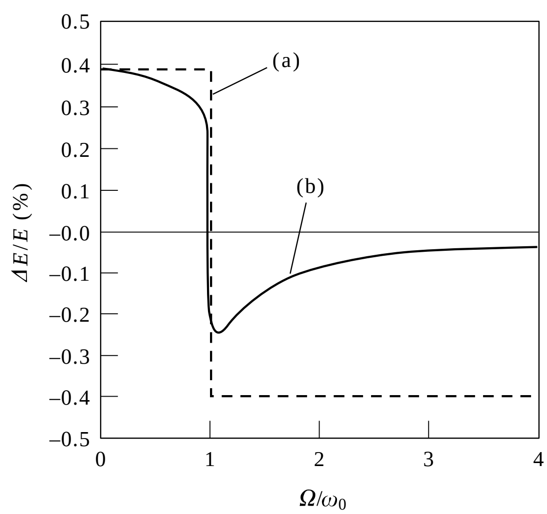

Figure 5. Energy transferral to the rotor per cycle due to the wedge microslip. (a) Constant normal force; (b) normal force increased by centripedal acceleration.

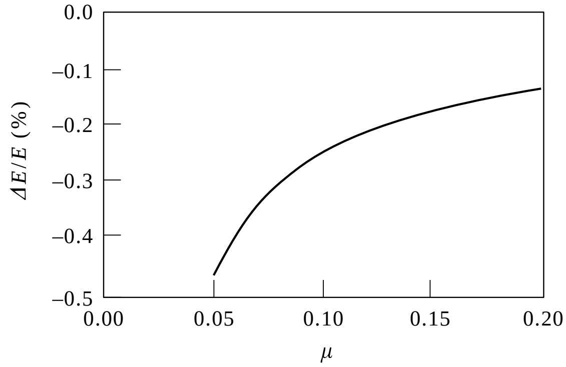

Figure 6. Energy transferral to the rotor per cycle due to the wedge microslip vs coefficient of friction when $\Omega/\omega_0 = 1{\cdot}1$.

3.1. WEDGE PROPERTIES

In Figure 5 the energy transferred is shown for one particular configuration of the wedge set. The parameters may, however, vary within wide ranges. In this section the parameter affecting the energy transferred for one rotational frequency ratio, namely $\Omega/\omega_0 = 1{\cdot}1$, will be studied.

In contrast to what can first be expected, the magnitude of the transferred energy decreases when the friction coefficient increases. This is shown in Figure 6. This is due to the fact that the energy transferred it proportional to the slip length squared but just linearly proportional to the friction force, and when the friction force is reduced the length of the slip zone is increased correspondingly.

The length of the wedge, or more accurately the position of the slip zone, seem to have a large influence on the energy transferred and, with reference to Figure 7, consequently the length of the wedge should be as large as possible. The slope of the shaft decreases the farther away from the middle of the shaft the slip zone is positioned. This decreases the strain in the wedge. In a real turbine generator the whole length of the wound part of the rotor consists of wedges, consequently the number of wedges in the axial direction decreases while the length of the wedges increases. This also decreases the energy transferred since the number of slip zones becomes smaller.

The wedge cross-section area contributes to the energy transferred in two ways. The larger the area is, the larger is the friction force that has to be transferred between the rotor

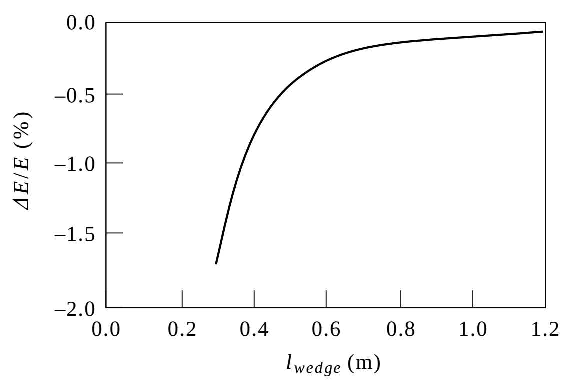

Figure 7. As Figure 6 except vs wedge length.

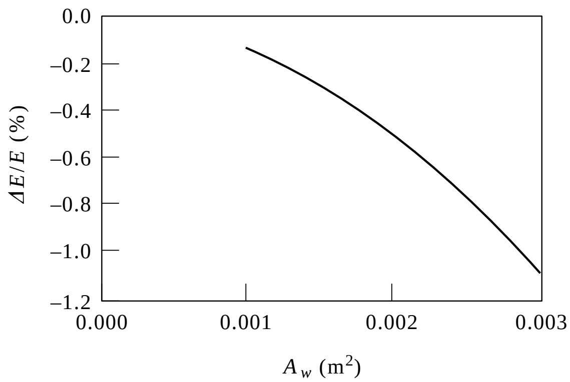

Figure 8. As Figure 6 except vs wedge cross-section area.

and the wedge and, consequentially, the larger will the slip zone and the energy transferred be. On the other hand the larger wedge cross-section area, the larger will the normal force due to the centripetal acceleration be.

In Figure 8 the energy transferred has been plotted for different wedge cross-section areas, but without changing the normal force. It is noted that the energy transferred increases when the cross-section area increases. It can be shown that the energy transferred is in principle independent of the equivalent rotor stiffness $E_r A_r$ as long as it is larger than the wedge stiffness $E_w A_w$.

As was discussed earlier the normal force on the wedge depends on the prestressed spring between the wedge and the conductors but also on the centrifugal forces. Their normal force can be increased either by increasing the prestress in the spring and/or reducing the slope of the wedge contact area: i.e. making the wedge more pointed. As shown in Figure 9, these will reduce the energy transferred.

From the results above the energy transferred can be written as

$$\Delta E \sim \frac{(E_w A_w)^2}{\mu N L_{wedge}^3}. \tag{5}$$

3.2. BEARING DAMPING

Up to now the bearings have been assumed to be rigid. Consequently no energy has been dissipated in the bearings. The instability can however be suppressed by a sufficient amount

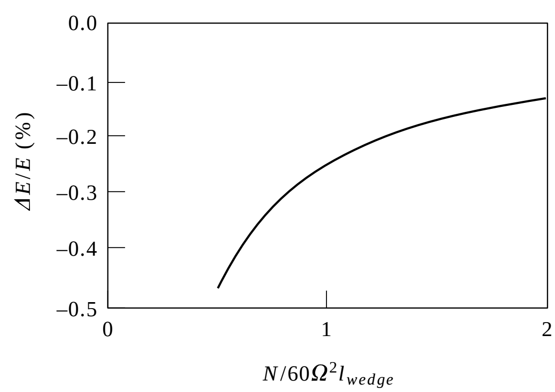

Figure 9. As Figure 6 except vs normal force.

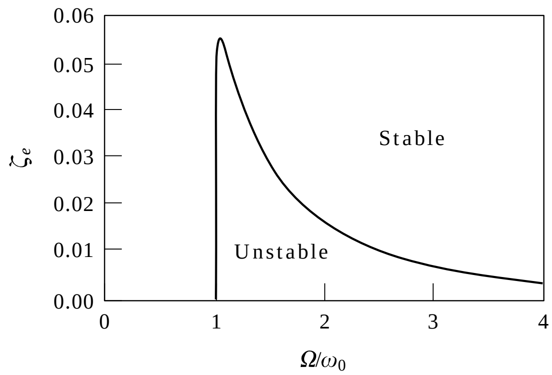

Figure 10. Bearing damping required to avoid instability. The bearing stiffnesses are $2k_e = 10k_i$.

of bearing damping. Figure 10 shows an example of how much bearing damping is needed to suppress the instability. The radius of the motion is $r = 0{\cdot}001$ m and the bearing damping factor is defined as

$$\zeta_e = \frac{2c_e}{2\omega_e m}, \tag{6}$$

where

$$\omega_e = \sqrt{\frac{(k_{ex} + k_{ey})k_i}{(k_{ex} + k_{ey} + k_i)m}}. \tag{7}$$

It is noted in Figure 10 that if the bearing damping factor, ζ_e, is larger than 0·057 the motion is stable for all rotational frequencies. The same analysis has been done for several different stiffness ratios and the result is shown in Figure 11. As can be seen in Figure 11 the bearing damping becomes more powerful the weaker the bearings are, for the simple reason that the motion decreases in the shaft, and so consequently does the dissipative energy.

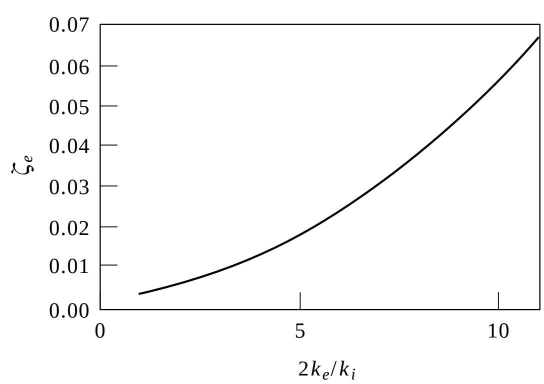

Figure 11. Bearing damping required to avoid instability.

4. CONCLUSION

The conclusions from this study can be summarized as follows.

The transferred energy decreases when the friction coefficient increases.

The energy transferred decreases when the length of the wedge increases or, more accurately, the farther away from the middle of the shaft the slip zone is positioned. It also decreases when the number of wedges becomes smaller although this is not as important.

The energy transferred also decreases when the normal force increases.

The energy transferred increases when the wedge cross-section area increases.

Within the range of the parameters in the study the results can be written as $\Delta E \sim [(E_w A_w)^2]/[\mu N L^3_{wedge}]$.

The stiffness of the bearings has a large influence on the required bearing damping to avoid instability. The larger the stiffness the larger the bearing damping.

REFERENCES

1. A. T. KIMBALL 1934 *General Electric Review* **158**, 216–228. Measurement of internal friction in a revolving deflected shaft.
2. E. J. GUNTER 1966 *SP*-113 NASA. Chapter 4. Dynamic stability of rotor-bearing systems.
3. D. E. BENTLEY 1972 72-*PET*-49. New York: ASME. The re-excitation of balance resonance regions by internal friction.
4. H. L. WETTERGREN and K.-O. OLSSON 1996 *Journal of Sound and Vibration* **195**(1), 75–84. Dynamic instability of a rotating asymmetric shaft with internal viscous damping supported in anisotropic bearings.
5. H. L. WETTERGREN 1994 *Fourth International Conference on Rotor Dynamics*, *Chicago*, *IL*, 7–9 September. IFToMM. Dynamic instability of composite rotors.
6. R. D. MINDLIN, W. P. MASON, J. F. OSMER and H. DERESIEWICZ 1952 1*st US National Congress of Applied Mechanics*, *Chicago*, *IL*, 203–208. New York: ASME. Effects of an oscillating tangential force on the contact surfaces of elastic spheres.
7. L. HAGMAN and S. BJÖRKMAN 1996 *Tribologia*, *Finnish Journal of Tribology* **15**(3), 52–65. Micro-slip measurements in contact subjected to normal and tangential loading.
8. H. L. WETTERGREN and G. CSABA 1998 *ASME Journal of Vibration and Acoustics*, in press. Dynamic instability of a turbine generator due to microslip.
9. H. L. WETTERGREN 1996 *Ph.D. Thesis*, *Linköping University*, *Sweden*. Rotordynamic analysis with special reference to composite rotors and internal damping.

APPENDIX: NOMENCLATURE

A_r area of the shaft
A_w area of the wedge cross-section
d_1, d_2 shaft diameters
E maximal potential energy to the rotor
E_r modulus of elasticity of the shaft
E_w modulus of elasticity of the wedge
EI_1, EI_2 bending stiffnesses of the shaft
F force in the shaft due to the wedge
F_x, F_y components of the applied force
F_w cross-section force in the wedge
f_f friction force per unit length
I_1, I_2 moment of inertia of the beam
k_{ex}, k_{ey} bearing stiffness
k_i equivalent shaft stiffness
l distance between the bearings
l_{wedge} length of the wedge
l_1, l_w, l_{slip} geometric properties of the shaft

M	bending moment
m	generalized mass of the shaft
m_{cond}	effective mass of the conductors
N	normal force on the wedge
n_{axial}	number of wedge sets
n_{circ}	number of wedges in each set
q	normal force per unit length
r	deflection of the rotor
r_{cond}	radius to the mass center of the conductors
r_{max}	maximum deflection of the shaft
t	time
x, y, z	Cartesian co-ordinate system
x_e, y_e	deflection in the bearing
α_{wedge}	angle between the wedge top surface and the normal force
β	stiffness ratio
δ_a	total slip length
ΔE	energy transferred to the rotor
μ	friction coefficient
ρ_{wedge}	density of the wedge material
ζ_e	bearing damping factors
Ω	rotational frequency
ω_e	resonance frequency
ω_0	vibrational frequency
ω_0^*	alteration frequency
E	maximal potential energy to the rotor